

# SEASONAL AND GLOBAL OZONE VARIATIONS WITH HETEROGENEOUS CHEMISTRY IN THE MARTIAN ATMOSPHERE.

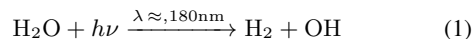
M. A. J. Brown, *School of Physical Sciences, The Open University, Milton Keynes, U.K. (megan.brown@open.ac.uk)*,  
M. R. Patel, S. R. Lewis, J. A. Holmes, J. Mason, A. Bennaceur, *The Open University, Milton Keynes, U.K.*, A. C. Vandaele, *Royal Belgian Institute for Space Aeronomy (BIRA-IASB), Brussels, Belgium*.

## Introduction

This study investigates the temporal and spatial effects of heterogeneous chemistry on ozone and hydroxyl radicals (OH and HO<sub>2</sub>, collectively known as HO<sub>x</sub>) using observed total column abundances (TCAs) of ozone, water ice, and water vapour, combined with Mars global climate model (MGCM) simulations with and without heterogeneous chemistry. We analyse the seasonal and latitudinal distribution of ozone and HO<sub>x</sub> to assess where heterogeneous chemistry influences trace gases, and the extent of this chemical impact. Analysing how the inclusion of heterogeneous chemistry affects ozone and HO<sub>x</sub> will help us understand the variation of HO<sub>x</sub> species, their sensitivity to water ice, and potentially improve simulations of ozone to be in better agreement with observations. Preliminary results show that the addition of heterogeneous chemistry increase the ozone TCA, although it does not account for all ozone deficit when compared to nadir observations.

Martian atmospheric chemistry is a key component to understanding crucial features on Mars, such as the water cycle, composition of the atmosphere, and the stability of carbon dioxide (CO<sub>2</sub>) [1]. These features can be investigated using trace gases in the atmosphere.

HO<sub>x</sub> are highly reactive trace species, and act as a catalyst in the recombination of carbon monoxide (CO) and molecular oxygen (O) to form CO<sub>2</sub>. As they are responsible for the stability of CO<sub>2</sub> in the atmosphere, the reactions HO<sub>x</sub> species undergo are important to clarify since they have the potential to impact multiple atmospheric species through trace amounts. Such investigations into the sensitivity of HO<sub>x</sub> on other species can be conducted through modelling. HO<sub>x</sub> are formed by the photolysis of water vapour;



where  $h$  is Planck's constant and  $\nu$  is the velocity of light at the wavelength given by  $\lambda$  [2]. Due to the high reactivity and very short lifetime, HO<sub>x</sub> cannot be easily measured directly. Instead, a combination of climate modelling and proxies are used to understand the temporal and spatial variation [3, 4, 5].

Ozone is often used as a proxy for HO<sub>x</sub> species, as its dayside lifetime is relatively short (2–3 hours), and it is sensitive both to the presence of HO<sub>x</sub> and to photochemistry. HO<sub>x</sub> react with ozone and destroy it, producing

more HO<sub>x</sub> species, which can then further react and destroy ozone, causing a set of chain reactions. Because of the direct production of HO<sub>x</sub> species from water vapour, there is a known photochemical anti-correlation between ozone and water vapour [1, 2, 6]. This relationship between ozone and water has been used in previous studies to investigate various chemical reactions which involve HO<sub>x</sub> species.

Comparing observed ozone to modelled ozone is often used to verify chemical reactions in models. Currently, ozone is underpredicted in GCMs, indicating missing or inaccurate chemical processes in models [3, 6, 7, 8]. One set of chemical reactions which have been offered as an explanation for this ozone deficit are heterogeneous chemical processes [5].

In the martian atmosphere, heterogeneous chemistry consists of trace species such as HO<sub>x</sub>, adsorbing onto the surface of dust and water-ice particles. In this study, we investigate the adsorption of HO<sub>x</sub> and hydrogen peroxide (H<sub>2</sub>O<sub>2</sub>) onto water ice. The water ice acts as a sink, preventing HO<sub>x</sub> from reacting with other species; the reduction in HO<sub>x</sub> results in an increase in ozone abundance as there are fewer HO<sub>x</sub> species to destroy ozone [7]. A proxy for detecting heterogeneous chemistry is via a positive relationship between ozone and water ice. In addition, heterogeneous chemistry can be investigated by comparing simulated ozone from global climate models (GCMs) with observations [5, 8].

## Nadir Observations

Ozone and water ice TCA data used in this study are from nadir observations from the the Ultraviolet and Visible channel (UVIS) [9] and spectrometer suite [10] of the NOMAD (Nadir and Occultation for Mars Discovery) spectrometer suite aboard the ExoMars Trace Gas Orbiter (TGO), and cover  $L_S = 0^\circ - 360^\circ$ , Mars Year 35 (Mason et al. in prep). Compared to vertical profiles derived from occultations measurements [6, 11], nadir observations have a wider spatial and temporal coverage and are thus more suitable for studying global and seasonal variations. Data are filtered by  $< 70^\circ$  SZA (solar zenith angle) and a relative error  $< 70\%$ . Observations are divided into bins of  $60^\circ L_S$  to capture the seasonal trend, and latitudinal bins of  $30^\circ$ . As there is little variation of ozone longitudinally, data are zonally averaged.

## Model Setup

The MGCM used for this study is that has been developed by the Open University Mars Modelling group, arising from a collaboration between the Laboratoire de Météorologie Dynamique (LMD), the Open University, the University of Oxford, and Instituto de Astrofísica de Andalucía [12]. The MGCM is run with 1920 dynamical timesteps per day, roughly 80 timesteps per hour, and uses a T31 spectral resolution, 70 vertical layers (scaled by pressure), 26 tracers, and is run both with and without heterogeneous chemistry.

## Cloud Microphysics

In the MGCM, there exists a ‘simple clouds’ scheme which uses the saturation water vapour limit to condense water vapour and form water ice. However, this scheme often overpredicts water ice, which, when used in conjunction with the heterogeneous scheme, tends to lead to an overprediction of ozone by a factor of two.

This overprediction results from the heterogeneous reactions use of the water ice surface area to calculate the rate of adsorption. Consequently, the overprediction of water ice produces higher adsorption reaction rates, leading to a greater abundance of  $\text{HO}_x$  adsorbed by water ice and, hence, a lower ozone destruction rate. In order to account for this, a cloud scheme containing water ice microphysics parametrizations is used in all MGCM simulations. The formation of water ice in this scheme is dependent on the cloud condensation nuclei (CCN) available, and allows for the supersaturation of water vapour to occur [13]. The cloud microphysics scheme produces a lower water ice abundance, which should decrease the impact of heterogeneous reactions on ozone.

## Chemistry

The chemical scheme used, ASIS, is taken from [14], using offline photochemical rates. It consists of 22 chemical tracers, and 60 chemical and photochemical reactions. The heterogeneous chemistry scheme used in the MGCM is taken from [8], and has been adapted by Brown et al. (in prep). Previously, studies have incorporated water ice only for calculating the adsorption rates of heterogeneous reactions [5, 8]. This work expands on Brown et al. (in prep) by improving the desorption of  $\text{HO}_x$  and  $\text{H}_2\text{O}_2$  by directly relating the desorption rate constant to the sublimation of water-ice clouds, as well as adapting the work from a 1-D model to a full GCM. We use the change in water ice due to sublimation to calculate the rate of desorption, which makes the heterogeneous reactions more sensitive to the vertical and temporal distribution of water ice. As a result, rapid changes in water ice abundance, such as the

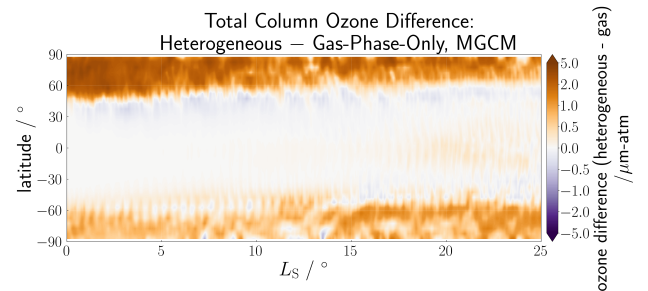


Figure 1: Difference in ozone TCA between simulations from the MGCM with and without heterogeneous chemistry (heterogeneous – gas-phase) between  $L_S = 0^\circ - 25^\circ$ . Data are zonally averaged. Note the non-linearity of the colourscale.

diurnal variations from night to day, are likely to have a greater impact on the chemical processes.

## Results

By comparing the ozone TCA simulated with and without heterogeneous chemistry, we study the global impact of heterogeneous chemistry on ozone and  $\text{HO}_x$ . This analysis expands on the investigation conducted by Brown et al. (in prep), by discussing the vertical distribution of ozone with heterogeneous chemistry and assessing the global impact of heterogeneous chemistry on ozone. We present results which show the global and temporal differences in ozone when simulated with and without heterogeneous chemistry, as well as the effects this has on  $\text{HO}_x$  species.

Observed and modelled TCA of ozone, and the observed relationship between ozone and water ice are used as a proxy for the occurrence of heterogeneous chemistry. Analysing the ozone and water ice TCA observations in conjunction with the simulated ozone and water ice gives an opportunity to show the strengths and weaknesses of including heterogeneous chemistry in a GCM. The addition of heterogeneous chemistry changes the  $\text{HO}_x$  distribution, which can be studied by the seasonal and local time variations in  $\text{HO}_x$  abundance.

## Seasonal Variation

Water-ice clouds have a seasonal variation, with the greatest abundances occurring at high latitudes during the local winter [15, 16]. As a result,  $\text{HO}_x$  species are expected to differ seasonally from the heterogeneous simulation to the gas-phase-only simulation.

Figure 1 shows the preliminary ozone difference between heterogeneous and gas-phase-only simulations across all latitudes, zonally averaged, from  $L_S = 0^\circ - 25^\circ$ . Orange indicates an increase in ozone abundance in the heterogeneous scheme with respect to the gas-

## REFERENCES

phase-only scheme, while purple indicates a decrease. Ozone TCA increases at higher latitudes, likely due to the formation of polar hood clouds during this time of the year.

From preliminary results, ozone TCA is still under-predicted at low latitudes during the aphelion season ( $L_S = 0^\circ - 90^\circ$ ). This is likely due to water vapour being overpredicted, which decreases ozone TCA as a result of increased  $\text{HO}_x$  abundance.

### Local Time

Water ice abundance varies with local time, with a higher abundance during the morning due to the condensation of water vapour overnight [17]. With the inclusion of heterogeneous chemistry, this variation is likely to impact the  $\text{HO}_x$  vertical distribution. As water ice sublimates,  $\text{HO}_x$  are released from the water-ice clouds. Combined with the photolysis of water vapour at the beginning of the day, the  $\text{HO}_x$  abundance may therefore be larger earlier in the sol than later in the evening. The change in the vertical distribution of  $\text{HO}_x$  species with heterogeneous chemistry could impact the ozone abun-

dance, which is typically lower during the morning than the evening [6].

### Conclusion

This work builds on the analysis from Brown et al. (in prep) to analyse the impact of heterogeneous chemistry on ozone in areas of high and low water vapour TCA. Nadir observations from TGO/NOMAD allow for a wide spatial and temporal coverage, which can be compared with simulations to investigate the underlying chemical processes in the atmosphere.

This investigation studies the global and temporal effects of heterogeneous reactions through observed and simulated ozone, and assesses the variation in  $\text{HO}_x$  with these chemical processes. The inclusion of heterogeneous processes has the potential to explain some of the ozone underprediction in GCMs [5, 8], and explore the sensitivity of  $\text{HO}_x$  in the presence of water ice on a local and seasonal timescale. From preliminary results, the addition of heterogeneous chemistry increases the ozone TCA at high latitudes ( $> 60^\circ$  N/S) at the northern spring equinox, due to the presence of the polar hoods.

### References

- [1] R. T. Clancy and H. Nair, "Annual (perihelion-aphelion) cycles in the photochemical behavior of the global mars atmosphere," *Journal of Geophysical Research: Planets*, vol. 101, no. E5, pp. 12785–12790, 1996.
- [2] F. Lefèvre, S. Lebonnois, F. Montmessin, and F. Forget, "Three-dimensional modeling of ozone on mars," *Journal of Geophysical Research: Planets*, vol. 109, no. E7, 2004.
- [3] F. Daerden, L. Neary, S. Viscardy, A. G. Muñoz, R. Clancy, M. Smith, T. Encrenaz, and A. Fedorova, "Mars atmospheric chemistry simulations with the gemars general circulation model," *Icarus*, vol. 326, pp. 197 – 224, 2019.
- [4] F. Montmessin and F. Lefèvre, "Transport-driven formation of a polar ozone layer on mars," *Nature Geoscience*, vol. 6, p. 930, 2013.
- [5] F. Lefèvre, J.-L. Bertaux, R. T. Clancy, T. Encrenaz, K. Fast, F. Forget, S. Lebonnois, F. Montmessin, and S. Perrier, "Heterogeneous chemistry in the atmosphere of mars," *Nature*, vol. 454, p. 971, 2008.
- [6] M. R. Patel, G. Sellers, J. P. Mason, J. A. Holmes, M. A. J. Brown, S. R. Lewis, K. Rajendran, P. M. Streeter, C. Marriner, B. G. Hathi, D. J. Slade, M. R. Leese, M. J. Wolff, A. S. J. Khayat, M. D. Smith, S. Aoki, A. Piccialli, A. C. Vandaele, S. Robert, F. Daerden, I. R. Thomas, B. Ristic, Y. Willame, C. Depiesse, G. Bellucci, and J.-J. Lopez-Moreno, "Exo-mars tgo/nomad-uvis vertical profiles of ozone: 1.

## REFERENCES

- seasonal variation and comparison to water,” *Journal of Geophysical Research: Planets*, vol. 126, no. 11, p. e2021JE006837, 2021. e2021JE006837 2021JE006837.
- [7] R. T. Clancy, M. J. Wolff, F. Lefèvre, B. A. Cantor, M. C. Malin, and M. D. Smith, “Daily global mapping of mars ozone column abundances with marci uv band imaging,” *Icarus*, vol. 266, pp. 112–133, 2016.
- [8] F. Lefèvre, A. Trokhimovskiy, A. Fedorova, L. Baggio, G. Lacombe, A. Määttänen, J.-L. Bertaux, F. Forget, E. Millour, O. Venot, Y. Bénilan, O. Korablev, and F. Montmessin, “Relationship between the ozone and water vapor columns on mars as observed by spicam and calculated by a global climate model,” *Journal of Geophysical Research: Planets*, vol. 126, no. 4, p. e2021JE006838, 2021. e2021JE006838 2021JE006838.
- [9] M. R. Patel, P. Antoine, J. Mason, M. Leese, B. Hathi, A. H. Stevens, D. Dawson, J. Gow, T. Ringrose, J. Holmes, S. R. Lewis, D. Beghuin, P. van Donink, R. Ligot, J.-L. Dewandel, D. Hu, D. Bates, R. Cole, R. Drummond, I. R. Thomas, C. Depiesse, E. Neefs, E. Equeter, B. Ristic, S. Berkenbosch, D. Bolsée, Y. Willame, A. C. Vandaele, S. Lesschaeve, L. De Vos, N. Van Vooren, T. Thibert, E. Mazy, J. Rodriguez-Gomez, R. Morales, G. P. Candini, M. C. Pastor-Morales, R. Sanz, B. Aparicio del Moral, J.-M. Jeronimo-Zafra, J. M. Gómez-López, G. Alonso-Rodrigo, I. Pérez-Grande, J. Cubas, A. M. Gomez-Sanjuan, F. Navarro-Medina, A. BenMoussa, B. Giordano, S. Gissot, G. Bellucci, and J. J. Lopez-Moreno, “Nomad spectrometer on the exomars trace gas orbiter mission: part 2—design, manufacturing, and testing of the ultraviolet and visible channel,” *Applied Optics*, vol. 56, no. 10, pp. 2771–2782, 2017.
- [10] A. C. Vandaele, J.-J. Lopez-Moreno, M. R. Patel, G. Bellucci, F. Daerden, B. Ristic, S. Robert, I. R. Thomas, V. Wilquet, M. Allen, G. Alonso-Rodrigo, F. Altieri, S. Aoki, D. Bolsée, T. Clancy, E. Cloutis, C. Depiesse, R. Drummond, A. Fedorova, V. Formisano, B. Funke, F. González-Galindo, A. Geminale, J.-C. Gérard, M. Giuranna, L. Hetey, N. Ignatiev, J. Kaminski, O. Karatekin, Y. Kasaba, M. Leese, F. Lefèvre, S. R. Lewis, M. López-Puertas, M. López-Valverde, A. Mahieux, J. Mason, J. McConnell, M. Mumma, L. Neary, E. Neefs, E. Renotte, J. Rodriguez-Gomez, G. Sindoni, M. Smith, A. Stiepen, A. Trokhimovsky, J. Vander Auwera, G. Villanueva, S. Viscardy, J. White-way, Y. Willame, M. Wolff, and t. N. Team, “Nomad, an integrated suite of three spectrometers for the exomars trace gas mission: Technical description, science objectives and expected performance,” *Space Science Reviews*, vol. 214, no. 5, p. 80, 2018.
- [11] A. S. J. Khayat, M. D. Smith, M. Wolff, F. Daerden, L. Neary, M. R. Patel, A. Piccialli, A. C. Vandaele, I. Thomas, B. Ristic, J. Mason, Y. Willame, C. Depiesse, G. Bellucci, and J. J. López-Moreno, “Exomars tgo/nomad-uvis vertical profiles of ozone: 2. the high-altitude layers of atmospheric ozone,” *Journal of Geophysical Research: Planets*, vol. 126, no. 11, p. e2021JE006834, 2021. e2021JE006834 2021JE006834.
- [12] F. Forget, F. Hourdin, R. Fournier, C. Hourdin, O. Talagrand, M. Collins, S. R. Lewis, P. L. Read, and J.-P. Huot, “Improved general circulation models of the martian atmosphere from the surface to above 80 km,” *Journal of Geophysical Research: Planets*, vol. 104, no. E10, pp. 24155–24175, 1999.
- [13] T. Navarro, J.-B. Madeleine, F. Forget, A. Spiga, E. Millour, F. Montmessin, and A. Määttänen, “Global climate modeling of the martian water cycle with improved microphysics and radiatively active water ice clouds,” *Journal of Geophysical Research: Planets*, vol. 119, no. 7, pp. 1479–1495, 2014.
- [14] D. Cariolle, P. Moinat, H. Teyssède, L. Giraud, B. Josse, and F. Lefèvre, “Asis v1.0: an adaptive solver for the simulation of atmospheric chemistry,” *Geoscientific Model Development*, vol. 10, no. 4, pp. 1467–1485, 2017.
- [15] J. L. Benson, D. M. Kass, A. Kleinböhl, D. J. McCleese, J. T. Schofield, and F. W. Taylor, “Mars’ south polar hood as observed by the mars climate sounder,” *Journal of Geophysical Research: Planets*, vol. 115, no. E12, 2010.
- [16] J. L. Benson, D. M. Kass, and A. Kleinböhl, “Mars’ north polar hood as observed by the mars climate sounder,” *Journal of Geophysical Research: Planets*, vol. 116, no. E3, 2011.
- [17] G. Liuzzi, G. L. Villanueva, M. M. Crismani, M. D. Smith, M. J. Mumma, F. Daerden, S. Aoki, A. C. Vandaele, R. T. Clancy, J. Erwin, I. Thomas, B. Ristic, J.-J. Lopez-Moreno, G. Bellucci, and M. R. Patel, “Strong variability of martian water ice clouds during dust storms revealed from exomars trace gas orbiter/nomad,” *Journal of Geophysical Research: Planets*, vol. 125, no. 4, p. e2019JE006250, 2020. e2019JE006250 2019JE006250.